MultiScience - XXX. microCAD International Multidisciplinary Scientific Conference
University of Miskolc, Hungary, 21-22 April 2016, ISBN 978-963-358-113-1

MICROSTRUCTURE CHARACTERISATION OF CASTED 17% Cr STAINLESS STEEL

Máté Sepsi[1], József Parti[2], Valéria Mertinger[3]
[1]undergraduate student, [2]PhD student, [3]professor
[1,3,4]University of Miskolc, Institute of Physical Metallurgy, Metalforming and Nanotechnology, Hungary, Miskolc – Egyetemváros

ABSTRACT

The evolving environmental requirements tend to decrease the pollutant emission and to decrease the fuel consumption demand changes in the applied materials. In this paper a Cr alloyed ferritic stainless steel developed for casting of an exhaust system component was investigated. The correlation between the concentration variables inside the standard regulation, the microstructure feature, and the hardness are experimentally shown.

INTRODUCTION

Tightening exhaust gas regulations and reducing fuel consumption by decreasing vehicle weight have come to be viewed as social requirements so the carmakers are redesigning the heavy components with thinner components to lower automotive weight and improve fuel efficiency. Accordingly the materials for the exhaust system components have also changed from conventional cast metals and carbon steel to various heat resistant alloys. The cast irons, stainless steels, and Ni-base super alloys have been considered as candidate materials of automotive exhaust systems. Among those candidates, ferritic stainless steels attracted a lot of attention due to their favorable low thermal expansion, sufficient mechanical strength at elevated temperature and excellent corrosion resistant properties [1,2]. The high corrosion resistance of these steels is due to alloying elements such as Cr, Ni and Mo. If the ferritic stainless steels are alloyed with strong carbide forming elements, such as Mo, Ti, V and Nb, hard phases, MC carbides can be obtained in the soft ferrite phase. The improvement of the properties of Fe–Cr–Ni cast steels is directly related to the development of the microstructure, which mainly consists of a ferritic matrix and carbides and/or dispersed intermetallics [3,4]. The steels generally have ferritic microstructure at room temperature if the ratio of Cr equivalent/Ni equivalent is higher than 1.8. Austenite persists to room temperature at extended concentrations of Ni equivalent. Therefore, the addition of a low Ni content seems to be an important alternative for improving mechanical properties. The presence of Ni in bcc microstructures is beneficial in increasing the notch-toughness and decreasing the ductile-to-brittle temperatures. It is considered that the iron transition temperature is subjected to a 10°C reduction for each 1 % Ni. In addition, Ni promotes austenite formation and also changes the microstructure feature. In spite of concentration similarity of the two phases in a multicomponent alloys the mechanical behaviors for example the hardness can be very different [5].
In the present work, the authors have investigated the microstructure features and the mechanical property, such as microhardness of ferritic stainless steels containing both ferrite (Si) and austenite (C, Mn, Ni) stabilizing and strong carbide-forming elements such as Cr, W. Light (LM) and scanning electron microscopy (SEM), energy dispersive spectrometry (EDS), and X-ray diffraction technique and micro and macro hardness tests were used.

DOI: 10.26649/musci.2016.022

EXPERIMENTAL

The material used in this study was high carbon ferritic stainless steel (1.4740W) which was melted in induction-melting furnace in industrial surrounding (Fig.1). The chemical compositions and the calculated equivalent numbers, and the ratio of the tested steels are shown in Table 1, compositions were measured by Spectrometer. The calculation was done as follows:

$$Cr_{eq}=Cr+2Si+1.5Mo+0.75W \quad (1)$$

$$Ni_{eq}=Ni+0.5Mn+30C \quad (2)$$

It can be stated that the standard requirements are fulfilled for all of the constitutions. The smallest equivalent ratio is 1,835 and the highest is 2,198 in case of H12 and H8 samples respectively.

Wedge-shaped specimens were poured into sand crucible. Size of the samples was 40 mm at the widest part, and 200 mm high. Cooling curves were measured in the specimens 5 and 15 mm thick sections by S type thermocouple and NI 9213thermocouple input (Fig.1).

Fig. 1. Pouring the sand crucible and the wedge shaped sample with the thermocouples (TC) branch joints and the sand crucible with TCs

Microstructures were studied by optical and scanning electron microscopy, Zeiss Axioimiger and Zeiss EVOMA10 equipped with EDAX were used. Specimens were etched in HNO3- HCl-H2O solute. XRD analysis was done using the Stresstech G3R centerless goniometer with Cr radiation, designed especially for residual stress and retained austenite measurements. 28KV accelerated voltage, 6mA filament, V filter and 5 mm in diameter collimator were used. The austenite volume fraction was calculated using the retained austenite module. Bruker D8 Advance diffractometer with Co radiation also was used to determine all of the presence phases and make the profile fit procedure more precisely.

Hardness and micro hardness were measured with a Vickers hardness tester Tukon 2100B with the load of 100 N and 0,1 N. Microstructure and hardness tests were performed at 5 and 15 mm wide sections and at the length section of the sample (in function of distance from the tip of wedge).

Table 1. The standard requirements and the measured chemical composition and equivalent numbers of tested steels, w/w %

	C	Si	Mn	Cr	Ni	W	Fe	Cr_{eq}	Ni_{eq}	Cr_{eq}/Ni_{eq}
min.	0,3	1,0	-	17	-	1,5	rest	-	-	-
max.	0,45	1,7	0,8	20	0,9	2	rest	-	-	-
H7	0,343	1,513	0,452	18,6	0,596	1,83	76,33	23	11,1	2,072
H8	0,3	1,481	0,42	19,08	0,553	1,709	75,98	23,3	10,6	2,198
H12	0,404	1,605	0,414	18,69	0,326	1,881	76,35	23,3	12,7	1,835

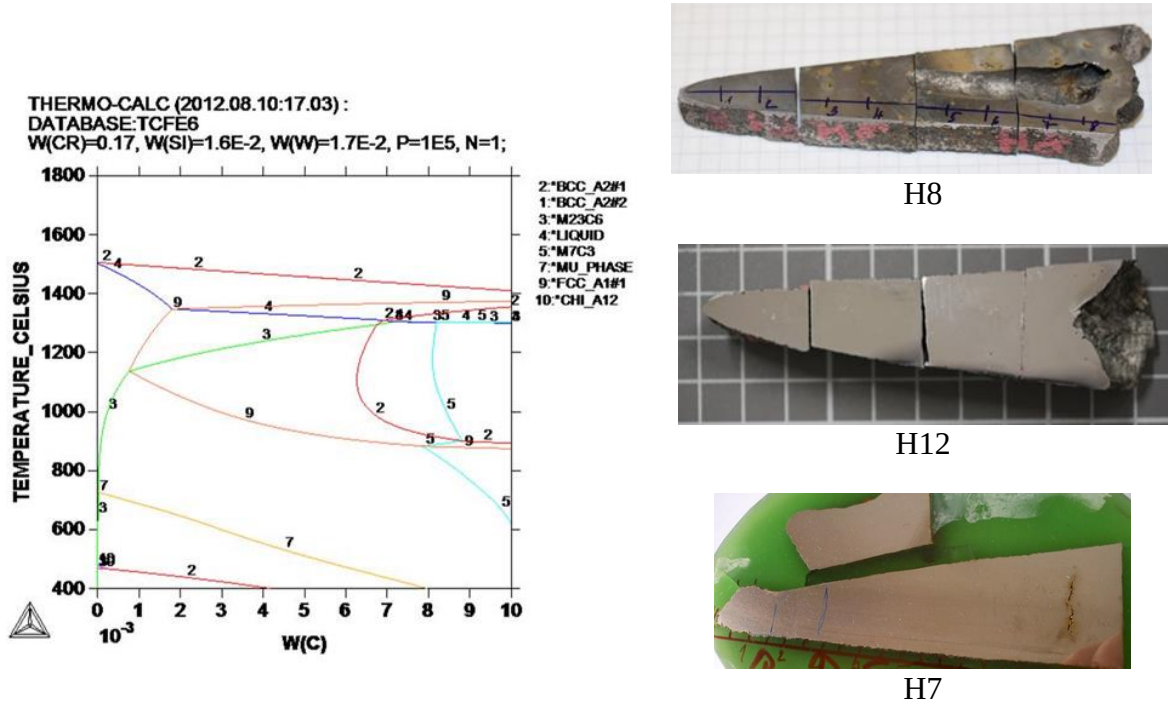

Fig.2. The calculated phase equilibrium diagram for the Fe, Cr, Si, W and C constitutions (Thermo-calc), and the half part of casted samples prepared for metallographic investigation

RESULTS

The Fig.2 shows the calculated equilibrium phase diagram section for the Fe, Cr, Si, W and C constitutions and the half part of casted samples prepared for metallographic investigation. It is evident that the microstructure can be very complex even in equilibrium state. If the significant or variable cooling rate and the micro segregation are also taking into account the complexity is increased. The recorded cooling curves at 5 and 10 mm section of wedge shaped casting H7 and H8 (Fig.3) show that small difference in the concentration resulted about 10 °C shifts in the liquidus temperature, while the solidus is unchanged. It is also clear that the local solidification time is longer in case of H8.

The Fig.4 shows the hardness distribution of the samples was investigated at 5 and 15 mm wide sections of H7 and the longitudinal sections. Result from the different sections (5 and 15 mm) represent similar hardness means that the different cooling rate does not result significant difference. Compering the different samples the H8 sample behaves smaller value than the two others, which are very similar. This difference in hardness causes problem during the machining so it can be the key issue in the necessity of the additional heat treatment technology, which increases the manufacturing costs.

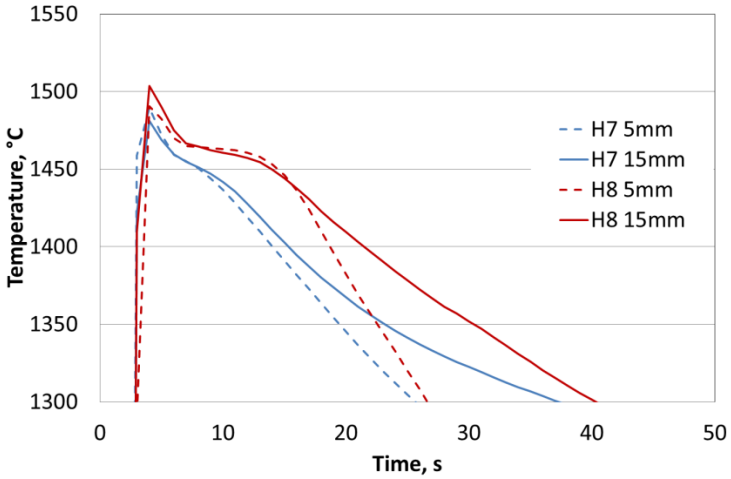

Fig. 3.The recorded cooling curves at the 5 mm and at the 10 mm section of samples H7 and H8

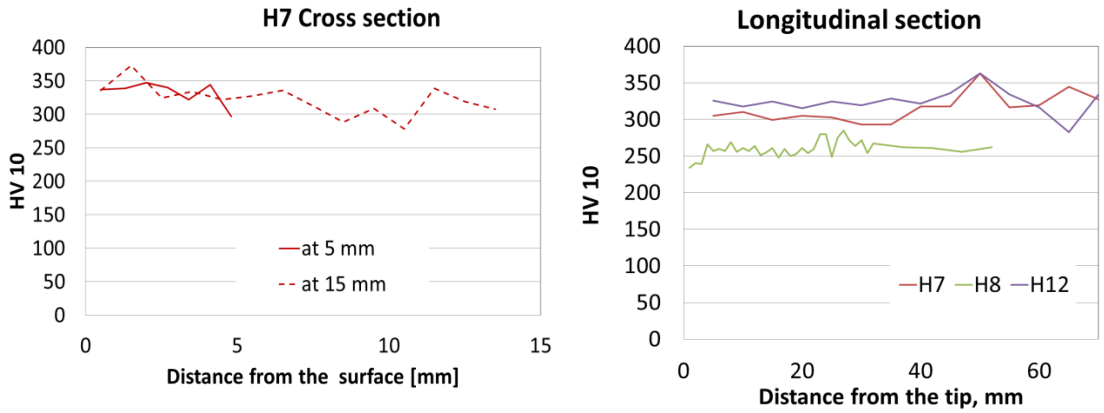

Fig.4. Hardness measurements

Fig. 5 shows the results of light microscopy. As it was estimated from the phase diagram, the microstructures show complex feature. Fine grains, fine precipitates in the grain boundary, two phase sections and solid solution parts with two different contrasts (light and dark) are observed. The dark grains surrounded by the precipitates and inserted into the lighter matrix. The volume fraction of the dark part is different in the three samples, highest at the H12. A more detailed investigation was performed using scanning electron microscopy. Selected area EDS was used to determine the chemical composition of the different phases. Result of the comparative analysis of the dark and light feature in the sample H8_1 and H8_4 can be seen in Fig. 6 and 7. It is clearly seen from the images that the different phases (dark, light) can be distinguished, but there is no significant difference in the chemical compositions. The very fine, bright grain boundary precipitation is probably W-Cr-Fe complex carbide (Fig. 7 area 4 and 5), while the lamellar precipitate inside the grain (area 6) is probably pure Cr carbide. The light and dark grains (area 1,2,3) represent smaller alloying elements' concentration.

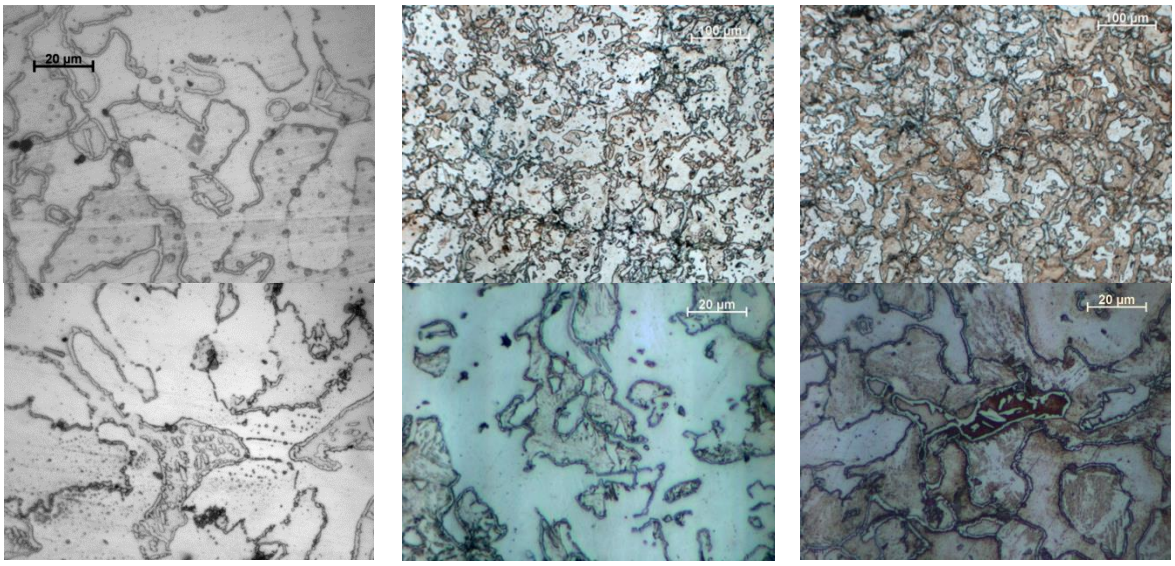

H7 H8 H12

Fig.5. Light microscopy features

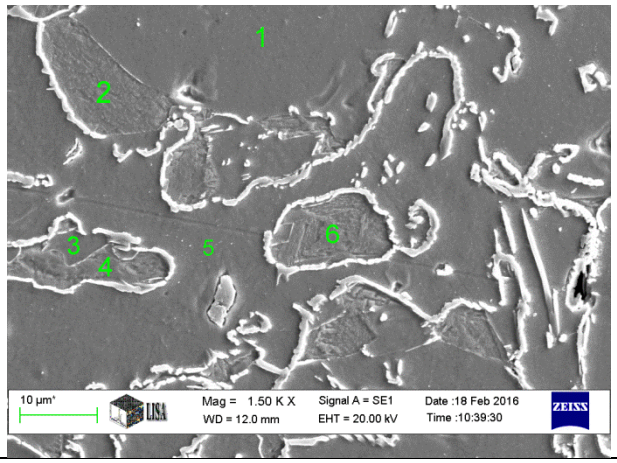

Element, w%							
Area	C	Si	Cr	Mn	Fe	Ni	W
1.	0,72	2,56	18,56	0,56	74,11	0,76	2,72
2.	0,93	1,93	18,59	1,01	72,74	1,21	3,58
3.	0,66	2,04	18,75	1	73,19	0,61	3,76
4.	0,74	2,37	19,29	0,68	72,82	0,76	3,34
5.	1,94	2,31	18,44	0,67	71,85	1,06	3,72
6.	1,38	2,12	18,98	0,77	73,88	0,76	2,1

Fig.6.Comparative EDS analysis of the dark (No.2,4,6) and of the light (No.1,3,5) features

In spite of the same concentration of the dark and light feature those behave very different hardness. The SEM pictures in Fig 8 a, b show the size of the indentations in the light and dark part respectively. The calculated HV0,01 also inserted; dark feature behaves higher value by more than 70.

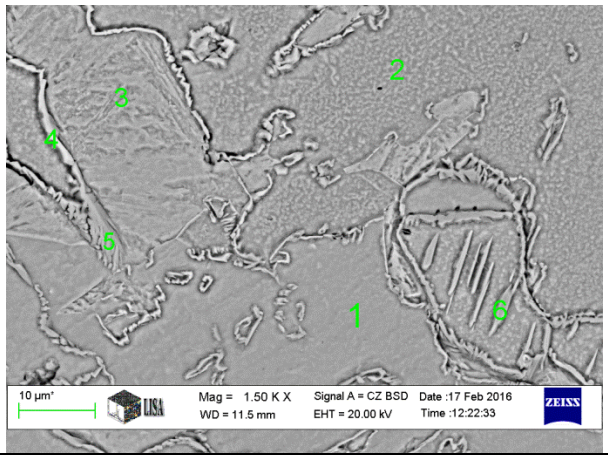

Element, w%							
Area	C	Si	Cr	Mn	Fe	Ni	W
1.	1,81	1,41	18,76	0,79	72,93	0,73	3,56
2.	1,25	1,58	19,39	0,61	73,21	0,65	3,31
3.	0,44	1,98	18,49	0,53	74,88	0,84	2,85
4.	4,63	1,16	40,91	0,35	45,44	0,86	6,65
5.	3,46	1,18	34,53	0,54	55,12	0,57	4,6
6.	3,79	0,59	65,82	0	26,18	0,64	2,98

Fig.7.Comparative EDS analysis of the features

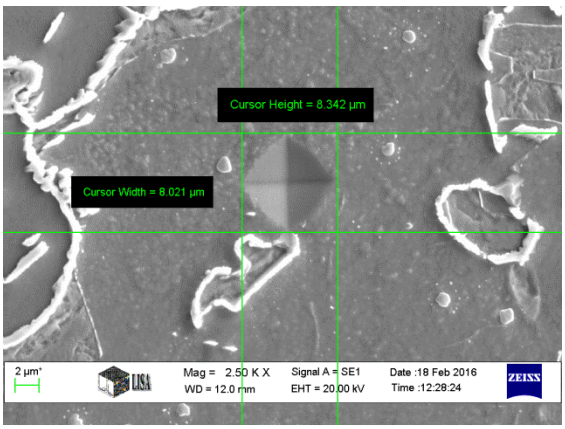

d_1=8,021µm, d_2=8,342µm, $HV_{0,01}$=277

a)

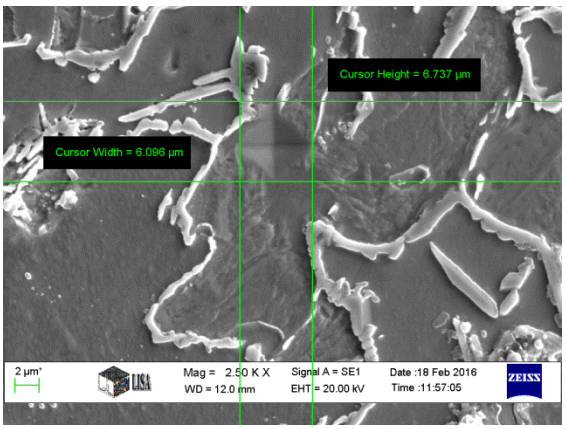

d_1=6,096µm, d_2=6,737µm, $HV_{0,01}$=450

b)

Fig.8.Comparative microhardness of the light (a) and the dark (b) parts

To distinguish the light and dark phase an XRD analysis was done. The evaluation of the full spectra distinguishes ferrite, austenite and minimum two kinds of carbides (Fig. 9). The ferrite (200) and (211) and the austenite (200) and (220) planes series were identified by the centreless X Stress G3R goniometer and the Xtronic software from the Stresstech which had been developed especially residual stress and retained austenite measurements. The diffracted peaks of sample H12_3 can be seen in the Fig 10. The background extraction was linear and the measured curve was fitted (blue curves) manually by Gauss distribution (red curves).The measurements were performed along the longitudinal axis in 6-8 points. The average results are in the Tabl.2. The calculation shows that the sample H12 contains more than 21 % austenite.

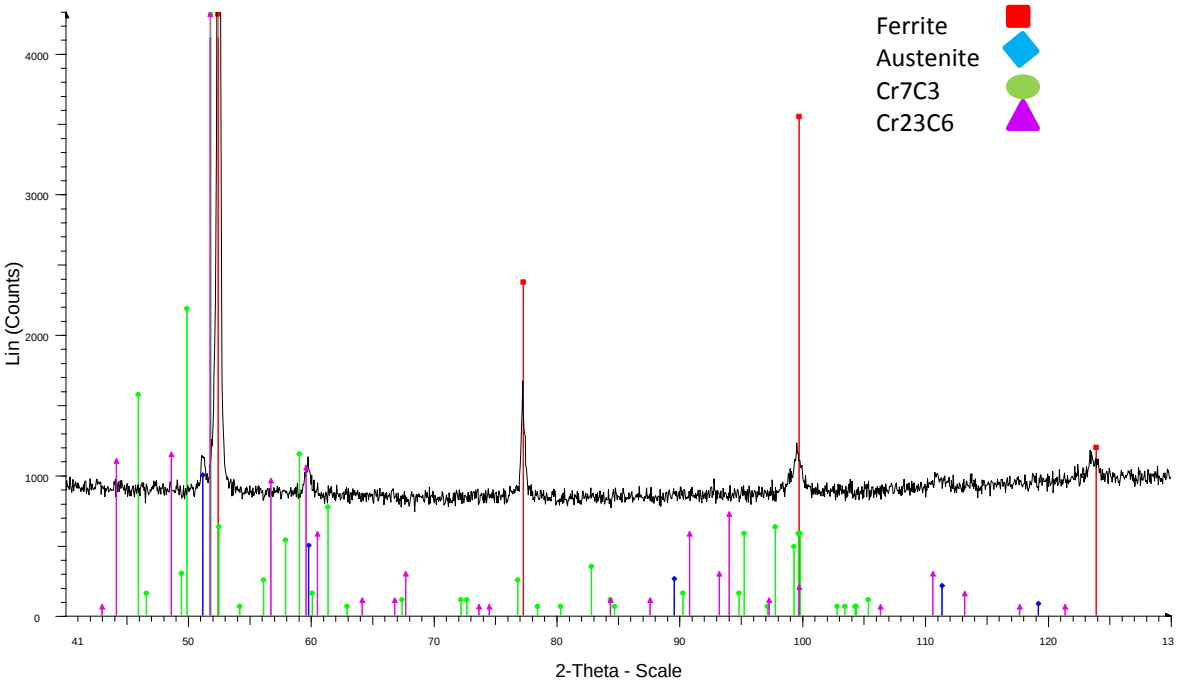

Fig.9.Full XRD spectra of samples H12_2a

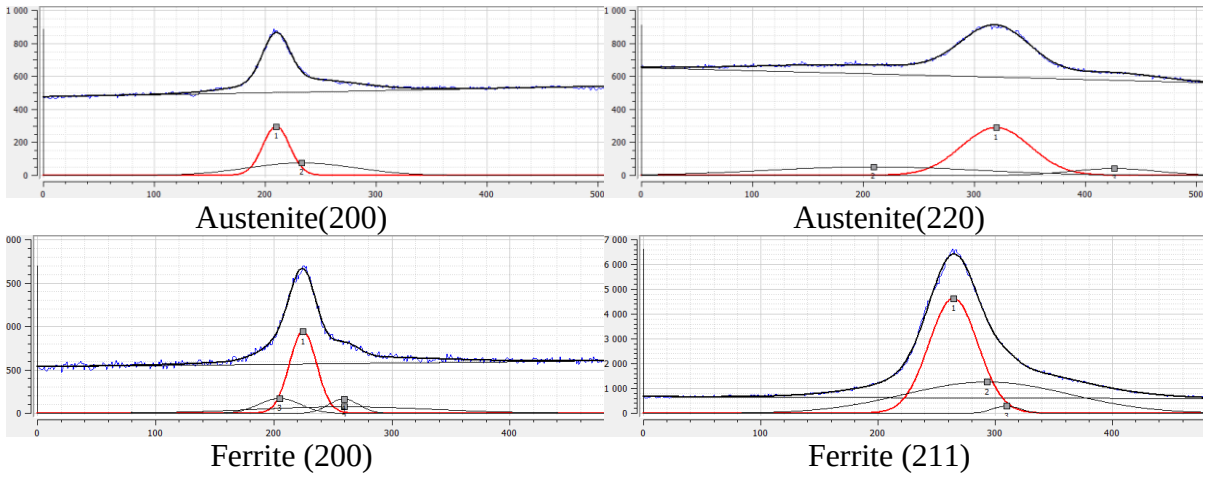

Fig.10. XRD spectra of samples H12_3 determined by position sensitive detectors

Table 2. The average austenite volume fraction of samples determined by XRD

Sample H7		Sample H8		Sample H12	
austenite %	±	austenite %	±	austenite %	±
14,8	5	8,4	4	21,4	3

SUMMARY

Wedge-shaped samples were poured into sand crucible to achieve different cooling rates of ferritic stainless steel alloyed by C, Cr, Si and W. The alloy is one of the new generation of ferritic stainless steels developed especially for the automotive gas exhaust system. The concentrations of the investigated samples were different but all fulfilled the standard

requirements. The Cr equivalent/Ni equivalent ratios are between 1,8 and 2,1. Cooling curves were recorded in two sections of the wedges. Hardness measurements were performed to determine the mechanical properties of the different microstructure constitutions. Light and electron microscopy with EDS system and XRD measurements were applied to describe the present phases. The summarized measured parameters are on the Fig 11. It is experimentally confirmed that the small shift of alloying element concentration (Creq/Nieq), even inside the standard requirements, results effect on the microstructure feature, especially the ferrite/austenite ratio which has a remarkable effect on the hardness of the sample. This effect can be so strong that the annealing heat treatment is needful.

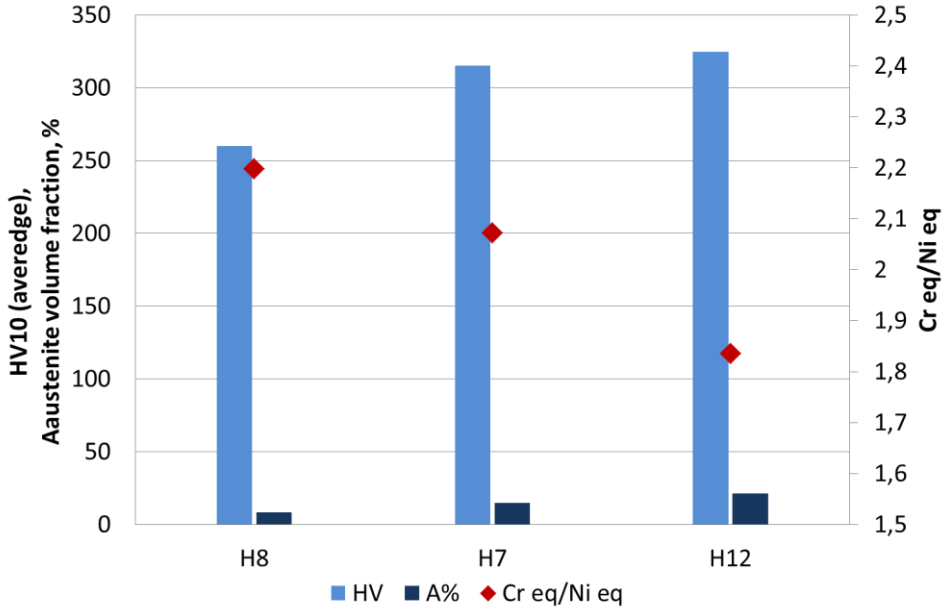

Fig.11Summarized measured parameters

ACKNOWLEDGEMENTS

This research was (partially) carried out in the framework of the Center of Applied Materials Science and Nano-Technology at the University of Miskolc. The authors thank to Dr. Erzsébet Nagy for the full XRD spectra and Árpád Kovács for the SEM pictures.

REFERENCES

[1] S. Bülbül, Y. Sun, Corrosion behaviors of high Cr–Ni cast steels in the HCl solution, Journal of Alloys and Compounds 498 (2010) 143–147
[2] S. J. Koa, Y. Kimb, High temperature fatigue behaviors of a cast ferritic stainless steel, Materials Science and Engineering A 534 (2012) 7– 12
[3] K.H. Lo, C.H. Shek, J.K.L. Lai, Recent developments in stainless steels. Materials Science and Engineering R 65, (2009) 39-104.
[4] N.H. Pryds, X. Huang, The Effect of Cooling Rate on the Microstructures Formed during Solidification of Ferritic Steel. Metallurgical and Materials Transactions, Volume 31A. (2000) 3155-3166
[5] H.P. Qu, Y.P. Lang, H.T. Chen, F. Rong, X.F. Kang, C.Q. Yang, H.B. Qin, The effect of precipitation on microstructure, mechanic properties and corrosion resistance of two UNS S44660 ferritic stainless steels, Materials Science and Engineering A 534 (2012) 436– 445